ACS Catalysis

RESEARCH ARTICLE

pubs.acs.org/acscatalysis

Synthesis of Methanethiol from Carbonyl Sulfide and Carbon Disulfide on (Co)K-Promoted Sulfide Mo/SiO_2 Catalysts

Oliver Y. Gutiérrez,[†] Christoph Kaufmann,[†] and Johannes A. Lercher*

Lehrstuhl für Technische Chemie 2, Technische Universität München, Lichtenbergstraße 4, D-85747 Garching, Germany

ABSTRACT: The catalytic properties of a series of (Co)K-promoted Mo sulfide catalysts supported on SiO_2 were explored in the synthesis of methanethiol from carbonyl sulfide (COS) and CS_2. MoS_2 was very active for the conversion of COS, but allowed only low yields of CH_3SH because of the parallel decomposition of COS to CO and H_2S and the reduction of CH_3SH to CH_4. CS_2, on the other hand, was completely converted to CH_3SH with high yield below 570 K on MoS_2. The formation of CH_4, however, dramatically decreased the yield of CH_3SH above 570 K. The addition of K^+ cations decreased the conversion of both reactants, but also reduced the rate of decomposition/reduction reactions. The doubly promoted CoK-Mo catalyst led to the highest conversions with moderate to high yields of methanethiol. We conclude that the addition of K^+ cations generates very weak adsorption sites, suppressing so the C−S bond cleavage. These sites catalyze, however, COS disproportionation. Accessible Co and Mo sites are part of the active sites for all reactions observed. All catalytic active sites are concluded to be on the edge of MoS_2 slabs.

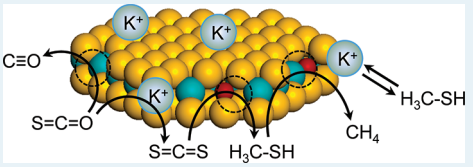

KEYWORDS: methanethiol, carbonyl sulfide, carbon disulfide, K−Co−Mo sulfide catalyst

1. INTRODUCTION

Methanethiol (methyl mercaptan, CH_3SH) is a key intermediate in the production of several important specialty chemicals such as methionine.[1] Thus, improving and developing new synthesis routes for methanethiol is of significant industrial interest. Large scale production of methanethiol is based on the thiolation of methanol.[1,2] However, it would be economically attractive to produce CH_3SH from less expensive reactants, such as carbon oxides, hydrogen sulfide, and hydrogen.

The synthesis of methanethiol from CO and CO_2 on transition metal sulfides supported on alumina was reported in the early work of Olin et al.,[3] whereas Mn- and W-based sulfide catalysts promoted with alkali metals were applied later.[4] The formation of methanethiol from mixtures of CO and H_2S was subsequently investigated over group Vb metal oxides supported on TiO_2 and Al_2O_3.[5−7]

In recent years, the synthesis of methanethiol from H_2S-containing synthesis gas (H_2S-syngas) on a variety of sulfide materials has received significant attention again.[8,9] The outstanding CO conversion and CH_3SH selectivity set the K-promoted Mo-catalyst apart from other evaluated catalysts.

A two-stage process for the synthesis of methanethiol was devised by the authors as reported in refs 10,11. The first stage consists in the liquid-phase reaction of elemental sulfur with CO-H_2 mixtures to form carbonyl sulfide (COS) and H_2S. In the second stage, a plug-flow reactor is used to synthesize methanethiol from mixtures of COS, H_2S, and H_2. The reactions in the second stage were catalyzed by Mo-sulfide catalysts containing substantial concentrations of potassium and being supported on SiO_2 and Al_2O_3.[11,12]

The two-stage approach allows also to better understand how the H_2S-syngas mixture reacts to form CH_3SH. From the mechanistic investigations it is concluded that COS undergoes disproportionation to CO_2 and CS_2 and that the latter is hydrogenated to methanethiol. The addition of high concentrations of potassium leads to the formation of a "K-decorated" MoS_2 phase that enhances the COS disproportionation, but inhibits undesired reactions. However, the sulfide catalyzed synthesis of methanethiol from H_2S-containing synthesis gas is far from being optimized and completely understood. Stimulated by reports in the literature[13] we compare here the impact of double promotion, that is, K−Co, on the methanethiol synthesis using COS and CS_2 as reactants aiming to provide a knowledge basis to improve catalysts for the synthesis of methanethiol from H_2S containing synthesis gas.

Cobalt was used as a second promoter because it is known to increase the reactivity of MoS_2 for hydrogenation.[14] Thus, a series of K- and CoK- promoted Mo catalysts supported on SiO_2 were synthesized, characterized, and explored with respect to the catalytic conversion of mixtures of COS or CS_2 with H_2S and H_2 to methanethiol.

2. EXPERIMENTAL SECTION

2.1. Catalyst Preparation. The oxide catalyst precursors were prepared by the incipient wetness impregnation of SiO_2 (AEROSIL 90, Degussa). Mo and K−Mo catalysts were prepared in a single impregnation step from aqueous solutions of ammonium heptamolybdate hexahydrated ($(NH_4)_6Mo_7O_{24}\cdot 6H_2O$, Aldrich, 99.9%) and potassium molybdate (K_2MoO_4, Sigma Aldrich, 98%), respectively. The resulting materials were dried at 353 K for 10 h and treated at 773 K in synthetic air for 12 h.

Received: September 6, 2011
Revised: October 6, 2011
Published: October 06, 2011

Table 1. Nominal and Experimental Metal Concentrations in the Oxide Materials[a]

material	Co (wt %) (nominal) experimental	K (wt %) (nominal) experimental	Mo (wt %) (nominal) experimental	BET surface area ($m^2 \cdot g^{-1}$)	pore volume ($cm^3 \cdot g^{-1}$)
SiO_2				88	0.15
Mo/SiO_2			(11.3) 13.3	78	0.12
KMo/SiO_2		(9.2) 8.8	(11.3) 11.4	50	0.06
$CoKMo/SiO_2$	(2.3) 1.8	(9.2) 8	(11.3) 11.5	25	0.03

[a] BET surface area and pore volume determined by N_2 physisorption.

The Co-containing catalysts were prepared by the impregnation of the K−Mo oxide material with an aqueous solution of cobalt nitrate hexahydrate ($Co(NO_3)_2 \cdot 6H_2O$, Fluka, 98%) followed by the same thermal treatment as described above. The molybdenum loading was 1.17 mmol per gram of material, whereas in the promoted catalysts the molar K/Mo and Co/Mo ratios were 2 and 0.33 respectively. The equivalent nominal compositions were 11.3, 9.2, and 2.3 wt % in Mo, K, and Co respectively. The oxide catalyst precursors are denoted as Mo/SiO_2, KMo/SiO_2, and $CoKMo/SiO_2$.

2.2. Characterization of the Catalysts. *Elemental Composition.* The molybdenum, potassium, and cobalt content of the oxide precursors were determined by atomic absorption spectroscopy (AAS) using a UNICAM 939 spectrometer.

Textural Properties. The textural properties of the oxide precursors were determined by nitrogen adsorption−desorption using a PMI automated BET sorptometer. The samples were degassed in vacuum at 673 K for 2 h before adsorption.

X-ray Diffraction. The oxide precursors and the sulfide catalysts after activity tests were characterized by X-ray diffraction (XRD). Samples of the used catalysts were measured after cooling down the reactor to room temperature in nitrogen flow. A Philips X'Pert Pro System (CuKα1-radiation, 0.154056 nm) operating at 45 kV and 40 mA was used for recording XRD. Measurements were carried out using a step size of 0.017° (2θ) and 115 s as count time per step.

NO and CO_2 Adsorption. NO and CO_2 adsorption were determined by a pulse technique using a flow apparatus equipped with a mass spectrometer (QME 200, Pfeiffer Vacuum). A sample of 0.1 g of catalyst was loaded in a quartz reactor and activated in situ under 10 vol % H_2S/H_2 at 673 K for 3 h. After cooling to the adsorption temperature, that is, 300 K for NO and 358 K for CO_2, the reactor was flushed with high purity He for 5 h. Pulses of 10 vol % of NO or CO_2 in He were introduced every 30 min. The total concentration of gas adsorbed was calculated as the sum of the uptakes per pulse.

2.3. Kinetic Measurements. The synthesis of CH_3SH from COS or CS_2 was investigated with the sulfide form of Mo, K−Mo, and Co−K−Mo catalysts. In the following the sulfide catalysts are denoted simply as MoS_2/SiO_2, $KMoS/SiO_2$, and $CoKMoS/SiO_2$. Prior to the activity tests, samples of 0.5 g of the catalysts (particle size 250−500 μm) were sulfided in 10 vol % H_2S/H_2 at 3 MPa and 673 K for 12 h. Kinetic measurements were carried out in an experimental setup comprising a semibatch reactor and a plug-flow reactor in serial arrangement. Pure H_2 or CO-H_2 mixtures were bubbled through liquid sulfur in the semibatch reactor to generate either COS-H_2S or H_2-H_2S mixtures as previously reported.[9,10] These mixtures were diluted with the necessary concentrations of H_2, N_2, and/or CS_2 and introduced to the plug-flow reactor, where the synthesis of methanethiol was performed. CS_2 was introduced to the setup using a Shimadzu LC-20AT pump and vaporized at 423 K before mixing with the gas flow.

Using COS as starting reactant, the typical composition of the feed was 7.33 vol % COS, 3.08 vol % H_2S, and 17 vol % H_2 in N_2 (H_2/COS ratio of 2.4). The effect of the H_2/COS ratio (2.4, 3.2, and 5.2) was explored with a fixed COS concentration of 8 vol % and a H_2/H_2S ratio of 4.3. In the synthesis of CH_3SH from CS_2, the composition of the feed was 8.5 vol % CS_2, 18 vol % H_2S, 50 vol % H_2, and 23 vol % N_2 (H_2/CS_2 ratio of 5.9). These compositions referred to the gas mixture used in the plug-flow reactor. All reactions were performed at a constant pressure of 3 MPa and temperatures ranging from 420 to 673 K. The gas hourly space velocity (GHSV), defined as (volumetric flow rate)·(volume of the catalyst bed)$^{-1}$ was kept constant 89 min^{-1} in all experiments by diluting the reactant mixture in N_2. Absence of transport artifacts was confirmed in preliminary experiments with varying catalyst particle size and flow rates. Samples were taken after reaching steady state in steps of 15 K and analyzed by gas chromatography using a Shimadzu GC 2014 equipped with a packed Haysep Q and a packed molecular sieve (13X) column.

3. RESULTS

3.1. Elemental Composition and Textural Properties. The metal concentration, surface area, and pore volume of the oxide catalysts are compiled in Table 1. The composition of metals in the oxide catalyst precursors is very similar to the metal concentration used in the precursor mixture during preparation. Table 1 shows that the surface area and pore volume of the materials decrease with the loading of metal oxides along with the increase in the density of the material. The Brunauer−Emmett−Teller (BET) surface area and the pore volume of $CoKMo/SiO_2$ was lower than what was expected after incorporating 1.8 wt % of Co, which may suggest that some pores were blocked in the parent material during the preparation procedure.

3.2. X-ray Diffraction Measurements. The X-ray diffractograms of the oxide precursors and the corresponding sulfide catalysts after the activity tests are shown in Figures 1a and 1b, respectively. The broad signal between 15 and 35° (2θ) evidence the amorphous nature of the silica support. A crystalline structure of silica would produce the main reflection at around 26° (2θ) instead of a broad signal (see for instance quartz, PDF no. 01-074-0764). All other reflections in the diffractogram of Mo/SiO_2 are attributed to orthorhombic MoO_3 (PDF no. 00-001-0706). The oxidic KMo/SiO_2 catalyst shows a mixture of K_2MoO_4 (PDF no. 00-024-0880) and $K_2Mo_2O_7$ (PDF no. 00-036-0347). For the $CoKMo/SiO_2$ catalyst, the addition of Co modifies the proportion of K- and Mo- oxides. The fraction of $K_2Mo_2O_7$ increases while that of K_2MoO_4 decreases. However, slight shifts of the peak positions compared with the reference PDF data could indicate a mixture of potassium molybdenum oxides with different stoichiometries.[15]

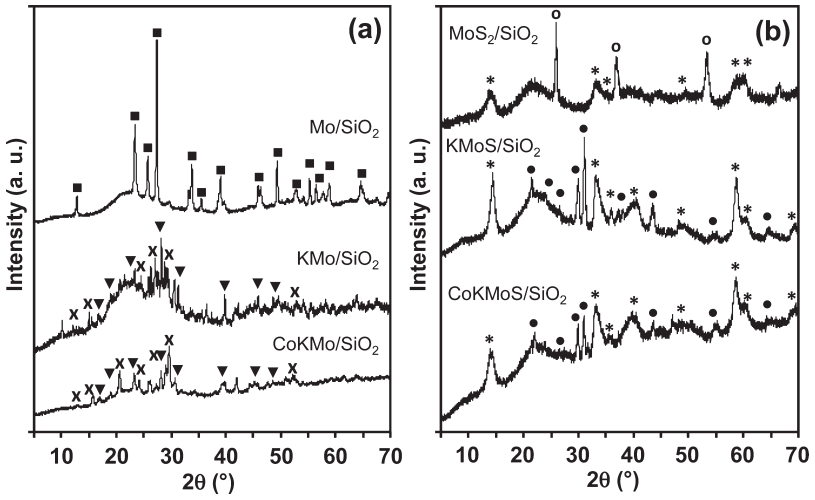

Figure 1. XRD diffractograms of the oxide precursors (a) and sulfided used catalysts (b). MoO_3 (■), K_2MoO_4 (▼), and $K_2Mo_2O_7$ (x) in (a); MoS_2 (*), MoO_2 (○), and K_2SO_4 (●) in (b).

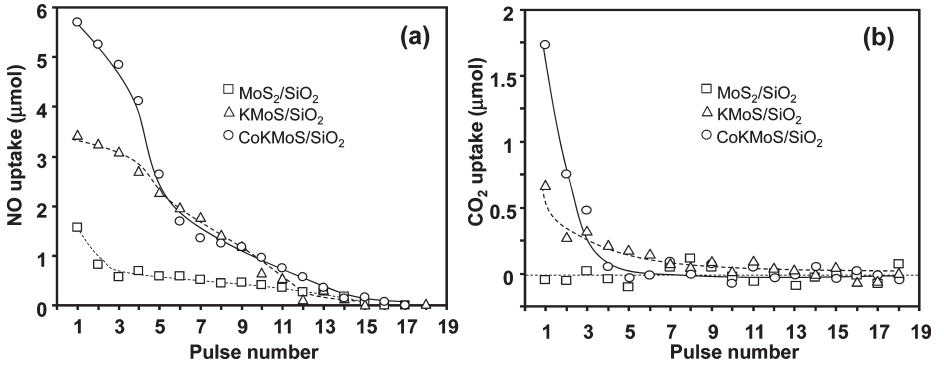

Figure 2. NO (a) and CO_2 (b) uptake at 300 and 358 K respectively on sulfided MoS_2/SiO_2 (□), $KMoS/SiO_2$ (Δ), and $CoKMoS/SiO_2$ (○).

Evidence of crystalline Co-containing phases is not found in the diffraction patterns, probably because the concentration of cobalt is too low.

The XRD of the sulfide catalysts collected after the activity tests are shown in Figure 1 b. Regardless of the oxide species present in the oxide precursor, all sulfided catalysts showed the presence of MoS_2 (PDF no. 00-024-0513) as the main crystalline phase. The diffractogram of the MoS_2/SiO_2 used catalyst showed some reflections corresponding to MoO_2 (PDF no. 00-033-0929) indicating incomplete sulfidation. In the sulfide and used $KMoS/SiO_2$ and $CoKMoS/SiO_2$ catalysts, the K_2SO_4 phase (PDF no. 00-003-0608) was also detected. This Mo-free phase formed during the reaction as discussed in ref 11.

3.3. NO and CO_2 Adsorption Measurements. The active sites in the sulfide catalysts were characterized by means of NO and CO_2 adsorption because NO adsorbs on exposed cations of MoS_2, whereas CO_2 selectively adsorbs on basic sites.[16,17] The uptake of NO and CO_2 per pulse on sulfide MoS_2/SiO_2, $KMoS/SiO_2$, and $CoKMoS/SiO_2$ is presented in Figure 2. Although there are marked differences in the starting uptakes of the samples, the uptake decreases to zero as the maximum adsorption capacity of the sample is reached. The NO uptake on the MoS_2/SiO_2 sample was rather low (69 μmol/g); however, the concentration of adsorbed NO increased significantly for the K-promoted catalyst (229 μmol/g) and was the highest for $CoKMoS/SiO_2$ (304 μmol/g).

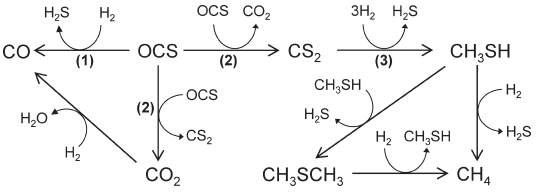

Figure 3. Reaction pathway for the production of CH_3SH from COS or CS_2. The main reaction steps are referred in the text as decomposition (1), disproportionation (2), and hydrogenation (3).

Only negligible concentrations of CO_2 were adsorbed on MoS_2/SiO_2, while 23 and 21 μmol/g of CO_2 were adsorbed on the $KMoS/SiO_2$ and $CoKMoS/SiO_2$ sulfide materials, respectively. Control experiments were also performed on pure SiO_2 after applying the same thermal treatment in H_2S/H_2 flow that was applied to the catalysts; adsorption of NO or CO_2 was not observed for pure SiO_2 carrier.

3.4. Comparison of Catalysts for the Synthesis of CH_3SH from COS. Previous studies of the synthesis of CH_3SH from COS implied that the reaction proceeds along the network presented in Figure 3.[11,12] COS is transformed to CO and H_2S via decomposition and in parallel, to CO_2 and CS_2 via disproportionation. CS_2 is hydrogenated to CH_3SH, whereas the reverse water gas shift reaction transforms CO_2 into CO. The

dx.doi.org/10.1021/cs200455k |ACS Catal. 2011, 1, 1595–1603

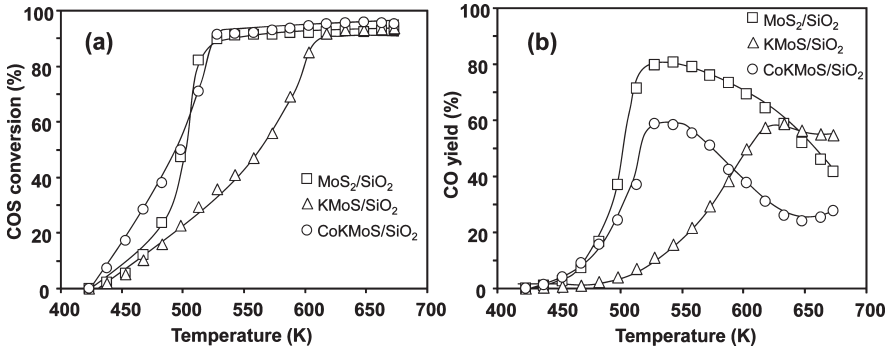

Figure 4. Conversion of COS (a) and yield of CO (b) on sulfided MoS_2/SiO_2 (□), $KMoS/SiO_2$ (Δ), and $CoKMoS/SiO_2$ (○). The feed contains 7.3 vol % COS and $H_2/COS = 2.4$ (3 MPa, GSHV = 89.2 min^{-1}).

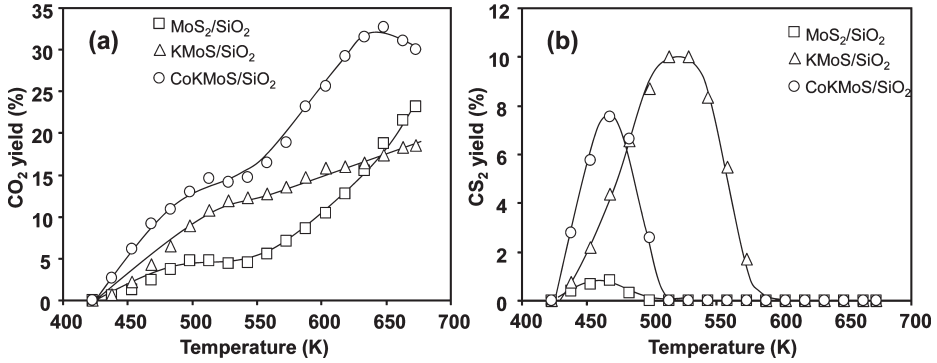

Figure 5. Yield of CO_2 (a) and CS_2 (b) on sulfided MoS_2/SiO_2 (□), $KMoS/SiO_2$ (Δ), and $CoKMoS/SiO_2$ (○). The feed contains 7.3 vol % COS and $H_2/COS = 2.4$ (3 MPa, GSHV = 89.2 min^{-1}).

secondary reactions involving CH_3SH lead to CH_4 and CH_3SCH_3 as suggested by the results of this work discussed below.

The synthesis of CH_3SH from COS was investigated over SiO_2-supported Mo, KMo, and CoKMo sulphide catalysts (see Figure 4a). With MoS_2/SiO_2 the conversion of COS increased rapidly from 12 to 80% between 473 and 508 K. With $KMoS/SiO_2$, the conversion of COS increased slower and did not reach the maximum value (>95%) until 623 K. The addition of cobalt increased the conversion of COS leading to the most active catalyst between 423 and 498 K. At temperatures higher than 498 K the conversions achieved with MoS_2/SiO_2 and $CoKMoS/SiO_2$ were both above 95%. The highest yield of CO was obtained on MoS_2/SiO_2 as shown in Figure 4b. Below 598 K, the yield of CO was higher on $CoKMoS/SiO_2$ than on $KMoS/SiO_2$ while the reverse was observed at higher temperature. On the three catalysts, the yield of CO increased with temperature to a maximum value before declining. The temperature for the maximum yield of CO varied from 543 K with MoS_2/SiO_2, to 633 K with $KMoS/SiO_2$ and 528 K on $CoKMoS/SiO_2$.

The yield of CO_2 is shown in Figure 5a. The highest yield was observed with $CoKMoS/SiO_2$ in the whole temperature range. With $KMoS/SiO_2$ the CO_2 yield was the second highest, whereas the lowest yield of CO_2 was observed with the unpromoted Mo sulfide catalyst. Three regions of the catalytic behavior can be distinguished in Figure 5a, that is, steady CO_2 yield increase (423−513 K), constant CO_2 yield (to 550 K), and finally CO_2 yield increase (>530 K). Very low yields of CS_2 were observed as shown in Figure 5b. The highest CS_2 yield (10%) was obtained with $KMoS/SiO_2$ at 523 K. Over the other systems, the maximum CS_2 yield was seen at 473 K, that is, 8% on $CoKMoS/SiO_2$ and just 1% on MoS_2/SiO_2.

A strong effect of the catalytic formulation was found on the yield of methanethiol (see Figure 6a). With MoS_2/SiO_2 the yield of methanethiol increased only to 7% at 518 K and then decreased again. With $KMoS/SiO_2$, the yield of methanethiol reached 18% at 603 K and did not significantly change with further increasing temperature. With $CoKMoS/SiO_2$, the yield of CH_3SH increased steeply from 423 to 513 K, then remained constant and increased again above 558 K reaching a maximum of 35% at 628 K. Figure 6b shows the yield of methane. The formation of CH_4 starts at 528 K on the unpromoted molybdenum catalyst, 633 K on $KMoS/SiO_2$, and 588 K on $CoKMoS/SiO_2$. In all cases, the yield of methane increased with reaction temperature.

3.5. Synthesis of CH_3SH from COS: Varying H_2/COS Ratio.

Clearly, the $CoKMoS/SiO_2$ system had the best performance with respect to the rate of COS conversion and the yield of methanethiol. Therefore, the effect of H_2/COS ratio was further studied on $CoKMoS/SiO_2$. Figure 7a shows that below 523 K, increasing H_2/COS ratio leads to an increase in the conversion of COS. Above that temperature, the conversion of COS was higher than 90%, regardless of the H_2/COS ratio applied. Similarly, the yield of CO increased by increasing the H_2/COS ratio as shown in Figure 7b.

The yield of CO_2 (Figure 8a) was independent of the H_2/COS ratio up to 483 K. Above that temperature, raising the H_2/COS ratio lowered the yield of CO_2. Formation of CS_2 was detected only at temperatures between 423 and 525 K and clearly decreased with increasing H_2/COS ratio as shown in Figure 8b.

dx.doi.org/10.1021/cs200455k |*ACS Catal.* 2011, 1, 1595–1603

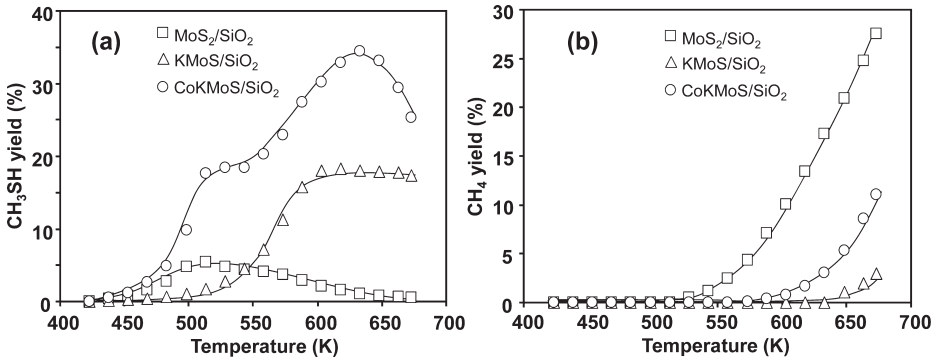

Figure 6. Yield of CH_3SH (a) and CH_4 (b) on sulfided MoS_2/SiO_2 (□), $KMoS/SiO_2$ (Δ), and $CoKMoS/SiO_2$ (○).The feed contains 7.3 vol % COS and H_2/COS = 2.4 (3 MPa, GSHV = 89.2 min^{-1}).

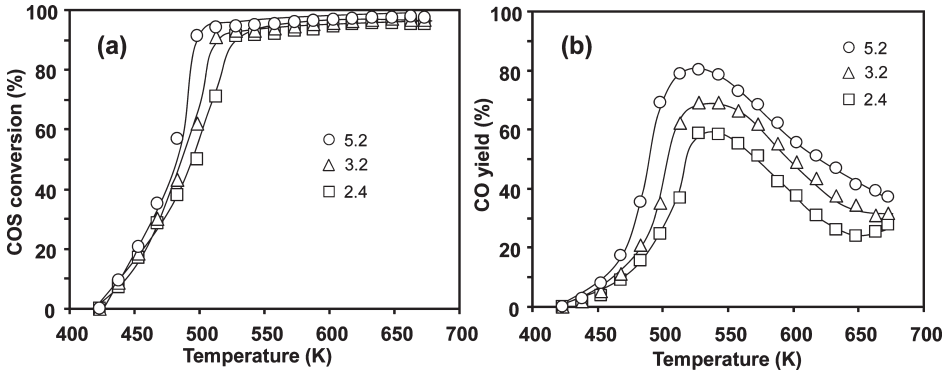

Figure 7. Conversion of COS (a) and yield of CO (b) on sulfided $CoKMoS/SiO_2$ at H_2/COS ratio of 5.2 (○), 3.2 (Δ), and 2.4(□). The feed contains 8 vol % COS and H_2/H_2S = 4.3 (3 MPa, GSHV = 89.2 min^{-1}).

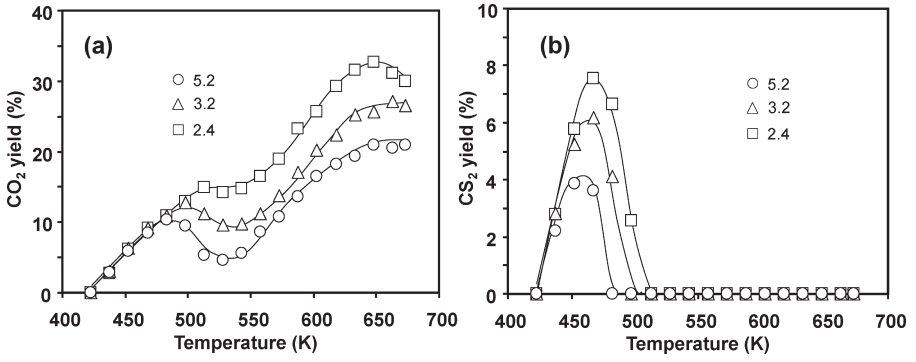

Figure 8. Yield of CO_2 (a) and CS_2 (b) on sulfided $CoKMoS/SiO_2$ at a H_2/COS ratio of 5.2 (○), 3.2 (Δ), and 2.4 (□). The feed contains 8 vol % COS and H_2/H_2S = 4.3 (3 MPa, GSHV = 89.2 min^{-1}).

The yield of CH_3SH increased by raising the H_2/COS ratio in the range 423−500 K (Figure 9a). Above this temperature, however, higher H_2/COS ratio led to lower yield of methanethiol. The yield of methane (Figure 9b) increased quickly above 598 K and was favored by increasing H_2/COS ratio.

3.6. Synthesis of CH_3SH from CS_2. Full conversion of CS_2 was achieved at 573 K as presented in Figure 10a. At lower temperatures, the highest CS_2 conversion was observed on $CoKMoS/SiO_2$ followed by the not promoted catalyst, and the $KMoS/SiO_2$ system led to the lowest CS_2 conversion. Figure 10b shows that the yield of methanethiol rapidly increased at temperatures above 573 K to a maximum value. On the unpromoted catalyst, the maximum yield of methanethiol was 84% at 548 K and then it decreased quickly to 0 at 623 K. On the K-containing catalyst the maximum CH_3SH yield of 98% was reached at 573 K followed by a steady decrease to 76% at 673 K. Using the $CoKMo/SiO_2$ catalyst, the maximum yield of CH_3SH (98%) was reached at 548 K, and it decreased to 58% at 673 K.

With all three catalysts, sulfided MoS_2/SiO_2, $KMoS/SiO_2$, and $CoKMoS/SiO_2$, only methane and dimethyl sulfide (CH_3SCH_3) were formed as byproducts in the synthesis of CH_3SH from CS_2. Figure 11a shows that for each catalyst the yield of CH_4 started

dx.doi.org/10.1021/cs200455k |*ACS Catal.* 2011, 1, 1595–1603

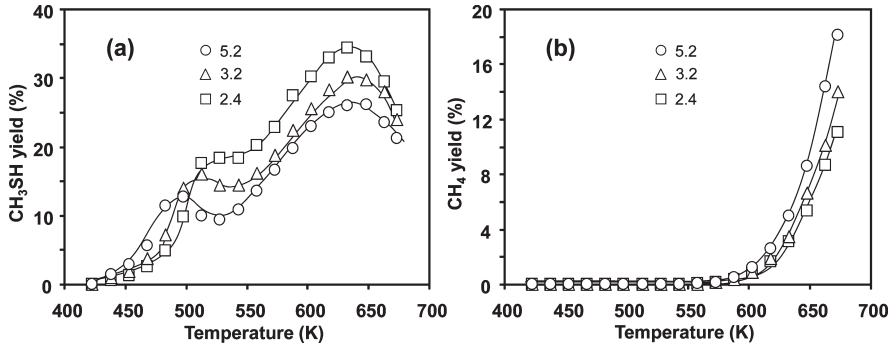

Figure 9. Yield of CH_3SH and CH_4 on sulfided $CoKMoS/SiO_2$ at a H_2/COS ratio of 5.2 (○), 3.2 (Δ), and 2.4 (□).The feed contains 8 vol % COS and H_2/H_2S = 4.3 (3 MPa, GSHV = 89.2 min^{-1}).

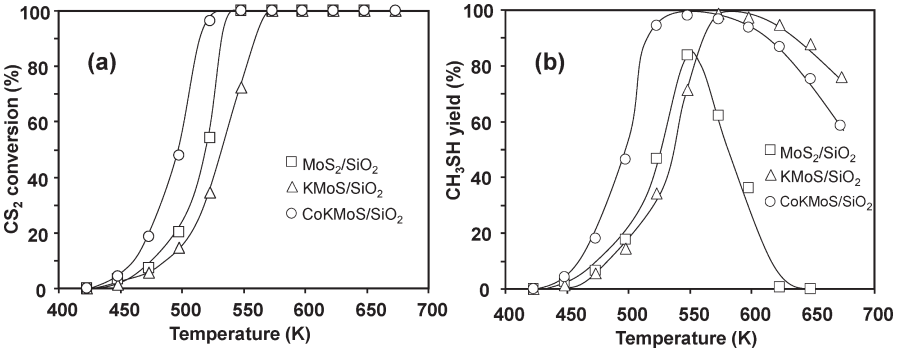

Figure 10. Conversion of CS_2 (a) and yield of CH_3SH (b) on sulfided MoS_2/SiO_2 (□), $KMoS/SiO_2$ (Δ), and $CoKMoS/SiO_2$ (○). The feed contains 8.5 vol % CS_2 and H_2/CS_2 = 5.9 (3 MPa, GSHV = 89.2 min^{-1}).

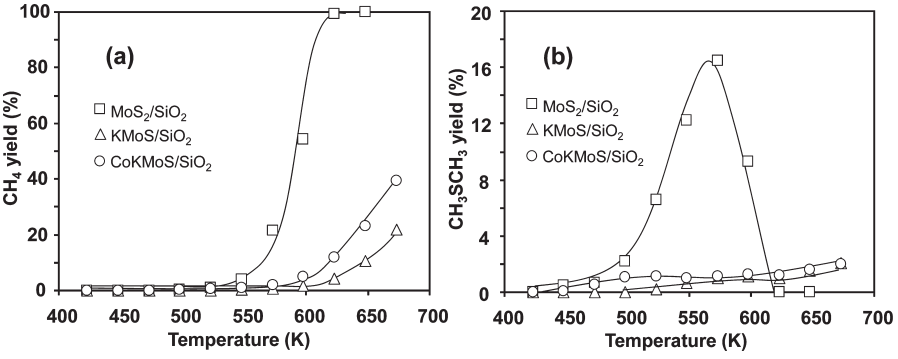

Figure 11. Yield of CH_4 (a) and CH_3SCH_3 (b) on sulfided MoS_2/SiO_2 (□), $KMoS/SiO_2$ (Δ), and $CoKMoS/SiO_2$ (○). The feed contains 8.5 vol % CS_2 and H_2/CS_2 = 5.9 (3 MPa, GSHV = 89.2 min^{-1}).

increasing at the temperature corresponding to the decline in the yield of CH_3SH. Thus, the decrease in CH_3SH yield at temperatures higher than 548 K was due to CH_3SH reduction to methane. With MoS_2/SiO_2, the yield of methane increased rapidly above 548 K and reached almost 100% at 623 K. The formation of methane was significantly decreased by the presence of potassium in the $KMoS/SiO_2$ catalysts. The addition of Co to the $KMoS/SiO_2$ catalyst, however, slightly increased the formation of CH_4 again. This methane formation on both promoted catalysts started at 598 K and increased up to 673 K to yield of 22 and 40% on $KMoS/SiO_2$ and $CoKMoS/SiO_2$, respectively. It is shown in Figure 11b that significant amounts of CH_3SCH_3 were observed only over MoS_2/SiO_2 where the CH_3SCH_3 yield increased up to 16.5% at 573 K and decreased at higher temperatures. Over the other systems the yield of CH_3SCH_3 was lower than 2% over the evaluated temperature range.

4. DISCUSSION

4.1. Effect of the Catalytic Formulation on the Synthesis of CH_3SH from COS. Let us analyze first the activity observed with MoS_2/SiO_2 and then describe the effects of the K- or Co and K-promotion. The conversion of COS which increases between 423 and 523 K is closely related to the yield of CO showing a parallel tendency. The yield of the other products, in contrast, remains rather low. This indicates that the decomposition of

dx.doi.org/10.1021/cs200455k |*ACS Catal.* 2011, 1, 1595–1603

COS to CO has the highest reaction rate between 423 and 523 K on MoS_2/SiO_2. Relatively stable yields of CO and CO_2 were observed between 523 and 548 K suggesting that in this narrow temperature range, the relative rates of COS disproportionation and decomposition are constant. At higher temperatures the linearly increasing yield of CO_2 coupled with a decreasing CO yield indicates that the COS disproportionation becomes faster than the decomposition. Hence, we conclude that the disproportionation of COS has a higher activation energy than its decomposition. The yield of CS_2 is zero above 500 K, that is, it was consumed faster than formed. Thus, we conclude that CS_2 hydrogenation to CH_3SH is faster than COS disproportionation.

The addition of potassium to the catalyst decreases the conversion of COS, but it does not slow down all reaction steps equally. The much lower yield of CO observed with $KMoS/SiO_2$ than with MoS_2/SiO_2 below 623 K suggests that the decomposition of COS is drastically reduced by potassium. The yield of CO_2, however, is much higher on the K-containing catalyst than on the unpromoted counterpart pointing to an increase in the rate of the COS disproportionation. In line with this statement, the yield of CS_2 is significantly higher with $KMoS/SiO_2$ than with MoS_2/SiO_2. The subsequent reactions are retarded by potassium to different extent. Note that the yield of CS_2 is negligible on MoS_2/SiO_2, whereas the yield of CH_3SH increases up to 5% at 500 K. This indicates that the hydrogenation of CS_2 to CH_3SH is fast. Interestingly, for the K-promoted catalysts the relatively high yield of CS_2 at 523 K is not accompanied by a high CH_3SH yield relative to the unpromoted system. Also, the formation of CH_4 ceased. Hence, the presence of potassium blocks or strongly retards the hydrogenation steps. The production of CH_3SH is less affected than the reduction to CH_4.

It is known that the reaction of syngas on MoS_2 yields hydrocarbons, whereas alcohols are selectively obtained on adding potassium to the catalytic formulation.[18,19] This observation seems to be analogous to the enhanced selectivity of H_2S-syngas to methanethiol on K-containing sulfides[9] as the carbon-heteroatom bonds are not cleaved in the presence of potassium. From another point of view, note that the hydrogenation of CS_2 to CH_3SH and the further reduction to CH_4 requires the cleavage of C−S bonds. From this perspective, the decelerating effect of potassium on the C−S bond cleavage observed in this work is consistent with investigations addressing hydrodesulfurization (HDS). The results of those investigations indicate that potassium reduces the HDS activity of Mo-sulfide catalyst for model molecules and real oil feeds.[20,21]

The formation of the $CoKMoS/SiO_2$ catalyst by adding cobalt increases the conversion of COS. Comparing the product yield observed with $KMoS/SiO_2$ and $CoKMoS/SiO_2$, the variation of the yields of CO, CS_2, and CO_2 show that the increased rates are due to the acceleration of two parallel reactions, that is, the decomposition and the disproportionation of COS. Interestingly, the yield of CO, remains lower on $CoKMoS/SiO_2$ than on MoS_2/SiO_2 (the yield of CO is even the lowest and the CO_2 yield the highest on $CoKMo/SiO_2$ of all catalysts above 600 K) indicating that potassium blocks the disproportionation pathway without cobalt reversing this blockage. The subsequent hydrogenation steps to CH_3SH and CH_4 are also accelerated by the cobalt promotion. In line with this accelerated disproportionation and subsequent hydrogenation, the yield of CS_2 reached a maximum value at lower temperatures than with other catalysts. In consequence, the yield of and the selectivity to CH_3SH is the highest with the double promoted MoS_2 catalyst. They decline slowly only above 650 K because of the enhanced reduction of CH_3SH to methane.

4.2. Effect of the Catalytic Formulation on the Synthesis of CH_3SH from CS_2. The reactions of CS_2 and H_2 on the unpromoted and the (Co)K-promoted catalysts confirm that the addition of potassium decreases the rate of CS_2 hydrogenation, whereas the presence of cobalt increases it, yielding only CH_3SH below 550 K. Above 550 K the CH_3SH yield drops with MoS_2/SiO_2 because of CH_4 formation. CH_3SH hydrogenation is nearly blocked with $KMoS/SiO_2$ indicating that the presence of K^+ cations blocks hydrogenation, while Co does hardly enhance CH_3SH hydrogenation, that is, it seems to remain less strongly adsorbed at the site of hydrogenation than on MoS_2/SiO_2. The significant formation of CH_3SCH_3 between 500 and 600 K with the latter catalyst and its disappearance in parallel to methane formation suggests that CH_4 is formed in a consecutive reaction from CH_3SCH_3 or as a parallel pathway (see Figure 3) on identical catalytic sites. The disappearance of these sites by addition of promoting atoms allows us to conclude that these sites are related to accessible Mo cations.

4.3. Effect of the H_2/COS Ratio on the Synthesis of CH_3SH on $CoKMo/SiO_2$. Increasing H_2/COS ratio led to the enhancement of the COS hydrodecomposition as seen from the increasing yield of CO, that is, $[COS + H_2 \rightarrow CO + H_2S]$. The increased rate of CO formation diminished the concentration of COS for the disproportionation reaction $[2COS \rightarrow CS_2 + CO_2]$. The positive influence of the hydrogen concentration suggests that all reactants are absorbed and that the two pathways follow the probability of finding a reaction partner on the sulfide surface.

Below 500 K higher partial pressures of H_2 enhanced the rate to CH_3SH $[CS_2 + 3H_2 \rightarrow CH_3SH + H_2S]$, while above accelerated rates of COS hydrodecomposition reduce the availability of CS_2, reducing so the rates to CH_3SH. It indicates that the energies of activation of the COS hydrodecomposition must be higher than that of CS_2 hydrogenation.

4.4. Role of the MoS_2 Phase and the Promoters. The X-ray diffractograms of the crystalline phases are reported from catalysts that were used in steady state operation after sulfidation of the oxide precursor. The catalytic experiments were also stopped to analyze the catalyst after different periods of reaction time, and the same XRD patterns for each catalyst were observed indicating the high stability of the investigated catalytic materials. In the active sulfide state all catalysts showed the MoS_2 phase. In addition MoO_2 was also detected with MoS_2/SiO_2, and the formation of K_2SO_4 was observed on the K-containing catalysts.

The X-ray diffractograms of the oxide precursor suggest that relatively large crystals (average diameter of 93 nm) are formed upon supporting MoO_3 on SiO_2. After the sulfidation procedure, the molybdenum is effectively reduced to Mo^{4+}. The large crystals, however, are not completely sulfided, which resulted in a mixture of MoS_2 and MoO_2, the latter species having an average diameter slightly above 80 nm. Therefore, it is reasonable to assume that the MoS_2 formation starts from the surface and that the reduction of molybdenum is not correlated with the sulfide formation. While the presence of K_2SO_4 is startling at first it is highly unlikely that it catalyzes any of the reactions discussed here, because it is highly stable and difficult to reduce.[22] Indeed, it has been observed that the formation of surface sulfate species decreased the conversion of CS_2 in reactions carried out on Al_2O_3 or TiO_2 supports.[23]

As the promoters, K or Co−K modify the behavior of the catalyst without changing the dominating MoS_2 phase. We conclude

in agreement with the literature that K^+ cations do not occupy specific sites in the catalyst, but are randomly distributed on the surface of support and the active sulfide phase.[8,10] Thus, some K^+ cations are associated with the sulfide and others are deposited on the support. It is also possible that not all supported MoS_2 is promoted by potassium. This random distribution of alkali promoter leads in consequence to the formation of two MoS_2 phases, that is, K-free and K-decorated MoS_2. K^+ cations not associated with MoS_2 agglomerates to form Mo-free crystalline species on silica, for example, K_2SO_4 as observed in this work. Interestingly, on Al_2O_3, K_2SO_4 does not form probably because of the stronger interaction of K^+ cations with alumina.[12]

Different catalytic behaviors have been proposed for the two different phases.[11,12] The K-free MoS_2 catalyzes mainly the COS decomposition and the hydrogenation of CH_3SH, whereas the K-promoted phase hinders these two reactions and promotes the disproportionation of COS. These assignments are consistent with what is observed in this work. The origin of this effect has been explained by assigning the role of adsorption center to K^+ cations. Accordingly, the NO adsorption increases from 69 to 230 μmol g^{-1} by adding 8.8 wt % of potassium in the studied catalysts. This increase of adsorption sites concentration is not reflected neither in the COS decomposition nor in the CS_2 hydrogenation. The only reaction enhanced with the K-promotion is the disproportionation of COS. This strongly suggests that the adsorption sites created by potassium differ from the Mo-coordinatively unsaturated sites (Mo-CUS). The K-containing sites are active for disproportionation, but reduce the concentration of Mo-CUS and so limit reactions catalyzed by accessible Mo cations. For a detailed discussion of the nature of the K-containing active sites see ref 12.

On the other hand, Co is a very specific promoter of Mo sulfide. It is well-known that Co interacts with MoS_2 forming the CoMoS phase, in which a fraction of Mo sites at the edges of the MoS_2 slab is replaced by Co.[24] This Co−Mo−S association is favored at Co/Mo molar ratios of around 0.5, whereas Co-sulfides form at higher contents of promoter. In this work an amount of Co below the maximum Co/Mo ratio for the formation of the Co−Mo−S phase was added to the Mo catalyst. Thus, we can assume that in the CoKMoS/SiO_2 catalyst the CoMoS phase is formed in agreement with the literature.[25] We cannot deduce from the present results whether or not Co incorporation occurs with preference on either MoS_2 or the K-decorated MoS_2. It is likely that cobalt decorates both MoS_2-like phases because all reaction steps are accelerated by Co promotion.

Considering that all reactions rates are accelerated and assuming that accessible Co is located at least in the nominal concentration at the edges of MoS_2 slabs, we deduce that all the reaction steps occur at the edges of MoS_2. To influence the catalytic performance of the MoS_2 phase, at least part of the K^+ cations must be located near the MoS_2 slab edges. Considering that K^+ enhances the O−S exchange,[12] it is highly likely that the K^+ cations enhance the exchange on the edge of MoS_2 slabs because these sulfur atoms are much more labile than sulfur in the basal planes.[26]

The influence of cobalt on MoS_2-based catalysts has been extensively studied for hydrotreating catalysts. Two main effects are attributed to Co-promotion, that is, increasing the concentration of CUS and facilitating the activation of H_2.[27] For the catalysts studied in this work, NO adsorption shows that the addition of Co increases the adsorption of NO from 230 to 304 μmol g^{-1}. Thus, the enhanced activity of the CoKMo/SiO_2 catalyst can be related to the increase of CUS in the MoS_2 edges[16] as it has been done for the synthesis of alcohols from syngas on K-doped Mo sulfides.[28]

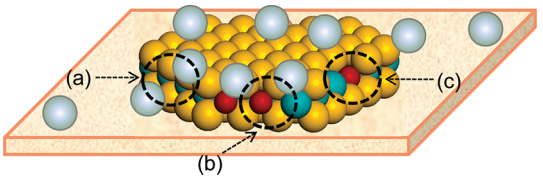

Figure 12. Schematic representation of a K- and Co-promoted MoS_2 slab. K^+ cations, Co, S, and Mo atoms are presented in white, red, yellow, and blue spheres, respectively. K^+-decorated site for COS disproportionation without Mo-CUS (a); potential active sites for all reactions promoted with Co and K^+ (b); Co-promoted hydrogenation and hydrogenolysis sites (c).

A schematic view of the K^+- and Co-promoted MoS_2 slabs is presented in Figure 12. While we assume that the K^+ cations are distributed over the material surface, only those deposited near the slab edges are relevant for the catalytic performance. The K-containing adsorption sites without Mo-CUS (a) would catalyze the disproportionation of COS. The sites containing both Co and K^+ (b) in principle catalyze COS disproportionation and decomposition as well as hydrogenation steps. However, the K^+ cations would act as weak adsorption sites decreasing the rate of hydrogenation by adsorbing more weakly the reaction intermediates. Finally, the MoS_2−CUS in the MoS_2 edge promoted only by Co would catalyze hydrogenation and C−S bond cleavage.

The enhancing effect of cobalt in the hydrogenation and hydrogenolysis steps is not surprising because the same effect has been observed in hydrotreating applications. The promotion of the disproportionation step can be attributed to the increase of oxygen and sulfur mobility in line with the known Co effect of decreasing the binding energy between Mo and the heteroatom.[29] On the other hand, the formation of CH_3SCH_3 on MoS_2/SiO_2 implies that two CH_3S- fragments adsorbed on adjacent Mo-CUS combine before desorption. However, the hydrogenolysis to methane is faster than the recombination to CH_3SCH_3 above 573 K. On the K-containing catalysts, the occurrence of two Mo-CUS would be less probable because of the blocking of such sites by K^+. Readsorption of CH_3SH, however, cannot be ruled out as one of the critical steps leading to the formation of CH_3SCH_3. K^+ cations would in that case reduce the probability that CH_3SH reacts further.

Final evidence of the different adsorption abilities of Mo-CUS and K^+ cations is given by CO_2 adsorption. On MoS_2/SiO_2, the uptake of CO_2 is negligible in accordance with reports that CO_2 does not adsorb on MoS_2.[17] In contrast, the sulfide KMo/Al_2O_3 catalyst adsorbs 23 μmol g^{-1}, which points to CO_2 adsorption involving the alkali atoms in agreement with ref 30. We speculate at present that such adsorption complexes have an sp^2 hybridized carbon atom. The adsorption of the same concentration of CO_2 on the sulfide CoKMoS/Al_2O_3 catalyst strongly suggests that the CO_2 interacts exclusively with K^+ cations, and not with CUS created by the incorporation of Co. The increased concentration of CUS on transition metals after Co-promotion is evidenced by the increase in the NO uptake by around 30%. This value is consistent with the increase of CUS concentration of 25−33% found in Al_2O_3-supported MoS_2 after promotion with Ni reported in refs 31,32.

5. CONCLUSIONS

The CH_3SH synthesis was carried out from COS/H_2 and CS_2/H_2 mixtures catalyzed with Mo, K−Mo, and Co−K−Mo sulfide catalysts supported on SiO_2. On unpromoted MoS_2, the (undesired) COS decomposition leading to CO and the hydrogenation of CH_3SH to CH_4 are favored and are associated with the presence of the highly reactive accessible Mo cations. The promotion with K^+, decorating supported MoS_2 and CoMoS particles, accelerates the COS disproportionation by providing sites for a facile exchange of oxygen and sulfur (presumably via surface mixed carbonates containing also sulfur atoms) and so reduce indirectly the formation of CO by COS decomposition. Note that also the addition of the more Lewis acidic Co cation increases the rate of C−S bond cleavage, therefore, it does not seem to stabilize carbonate structures.

The promotion with potassium also retards all steps requiring hydrogen, so decreasing the formation of methane. However, the formation of CH_3SH is affected less leading to the optimum yield. Adding Co accelerates all individual steps in the reaction network. The CH_4 formation rate is only enhanced at higher temperatures hardly limiting the temperature window in which high yields of methanethiol are achievable. Minimizing the H_2 partial pressure allows further optimization of the CH_3SH selectivity.

AUTHOR INFORMATION

Corresponding Author

*Fax: +49/89/28913544. E-mail: johannes.lercher@ch.tum.de.

Author Contributions

†The first two authors contributed equally to this work.

Funding Sources

The authors gratefully acknowledge Evonik Industries AG (Germany) for partial financial support of this work.

ACKNOWLEDGMENT

The authors gratefully acknowledge Evonik Industries AG (Germany) for fruitful discussions.

REFERENCES

(1) Sauer, J.; Boeck W.; von Hippel, L.; Burkhardt, W.; Rautenberg, S.; Arntz, D.; Hofen, W. U.S. Patent 5 852 219, 1998.

(2) Mashkin, V.; Kudenkov, V.; Mashkina, A. *Ind. Eng. Chem. Res.* **1995**, *34*, 2964–2970.

(3) Olin, J.; Buchholz, B.; Loev, B.; Goshorn, R. U.S. Patent 3 070 632, 1962.

(4) Haines, P. U.S. Patent 4 449 006, 1984.

(5) Ratcliffe, C.; Tromp, P. U.S. Patent 4 668 825, 1987.

(6) Ratcliffe, C.; Tromp, P.; Wachs, I. U.S. Patent 4 570 020, 1985.

(7) Mul, G.; Wachs, I.; Hirschon, A. *Catal. Today* **2003**, *78*, 327–337.

(8) Zhang, B.; Taylor, S.; Hutchings, J. *New J. Chem.* **2004**, *28*, 471–476.

(9) Chen, A.; Wang, Q.; Li, Q.; Hao, Y.; Fang, W.; Yang, Y. *J. Mol. Catal A: Chem.* **2008**, *283*, 69–76.

(10) Kaufmann, C.; Gutiérrez, O.; Zhu, Y.; Lercher, J. *Res. Chem. Intermed.* **2010**, *36*, 211–225.

(11) Gutiérrez, O.; Kaufmann, C.; Hrabar, A.; Zhu, Y.; Lercher, J. *J. Catal.* **2011**, *280*, 264–273.

(12) Gutiérrez, O.; Kaufmann, C.; Lercher, J. *ChemCatChem* **2011**, *3*, 1480–1490.

(13) Chen, A.; Wang, Q.; Hao, Y.; Fang, W.; Yang, Y. *Catal. Lett.* **2007**, *118*, 295–299.

(14) Topsøe, H.; Clausen, B.; Massoth, F. *Hydrotreating Catalysis Science and Technology*; Springer-Verlag: New York, 1996.

(15) Bian, G.; Fu, Y.; Ma, Y. *Catal. Today* **1999**, *51*, 187–193.

(16) Topsøe, N.; Topsøe, H. *J. Catal.* **1982**, *77*, 293–296.

(17) Zmierczak, W.; Qader, Q.; Massoth, F. *J. Catal.* **1987**, *106*, 65–72.

(18) Lee, J.; Kim, S.; Lee, K.; Nam, I.; Chung, J.; Kim, Y.; Woo, H. *Appl. Catal., A* **1994**, *110*, 11–25.

(19) Surisetty, V.; Hu, Y.; Dalai, A.; Kozinski, J. *Appl. Catal., A* **2011**, *392*, 166–172.

(20) Kelly, J.; Ternan, M. *Can. J. Chem. Eng.* **1979**, *57*, 726–733.

(21) Verbruggen, N.; Knözinger, H. *Langmuir* **1994**, *10*, 3148–3155.

(22) Kasznoyi, A.; Hronec, M.; Delahay, G.; Ballivet-Tkatchenko, D. *Appl. Catal., A* **1999**, *184*, 103–113.

(23) Laperdrix, E.; Justin, I.; Costentin, G.; Saur, O.; Lavalley, J.; Aboulayt, A.; Ray, J.; Nédez, C. *Appl. Catal., B* **1998**, *17*, 167–173.

(24) Topsøe, N.; Topsøe, H. *J. Catal.* **1983**, *84*, 386–401.

(25) Iranmahboob, J.; Hill, D.; Toghiani, H. *Appl. Catal., A* **2002**, *23*, 99–108.

(26) Tauster, S.; Pecoraco, T.; Chianelli, R. *J. Catal.* **1980**, *63*, 515–519.

(27) Moses, P.; Hinnemann, B.; Topsøe, H.; Nørskov, J. *J. Catal.* **2009**, *268*, 201–208.

(28) Bao, J.; Fu, Y.; Bian, G. *Catal. Lett.* **2008**, *121*, 151–157.

(29) Byskov, L.; Nørskov, J.; Clausen, B.; Tøpsoe, H. Sulphur bonding in transition metal sulphides and MoS_2 based structures. In *Transition Metal Sulphides − Chemistry and catalysis*; Kluwer Academic Publishers: Dordrecht, Netherlands, 1998.

(30) Karolewski, M.; Cavell, R. *Surf. Sci.* **1989**, *219*, 261–276.

(31) Hrabar, A.; Hein, J.; Gutiérrez, O.; Lercher, J. *J. Catal.* **2011**, *281*, 325–338.

(32) Gutiérrez, O.; Klimova, T. *J. Catal.* **2011**, *281*, 50–62.